Electrochimica Acta 152 (2015) 93–100

Contents lists available at ScienceDirect

Electrochimica Acta

journal homepage: www.elsevier.com/locate/electacta

Alkaline membrane fuel cells with *in-situ* cross-linked ionomers

Yongjun Leng [a], Lizhu Wang [b], Michael A. Hickner [b], Chao-Yang Wang [a,b,*]

[a] Electrochemical Engine Center, Department of Mechanical and Nuclear Engineering, The Pennsylvania State University, University Park, Pennsylvania 16802, United States

[b] Department of Materials Science and Engineering, The Pennsylvania State University, University Park, PA 16802, USA

ARTICLE INFO

Article history:
Received 27 May 2014
Received in revised form 22 October 2014
Accepted 8 November 2014
Available online 11 November 2014

Keywords:
Alkaline membrane fuel cell (AMFC)
in-situ cross-linking
ionomer
net water transport coefficient

ABSTRACT

Improving cell performance and durability through both new materials and membrane electrode processing optimization is needed for the commercialization of alkaline membrane fuel cell (AMFC) technologies. In this work, we adopted an *in-situ* cross-linking strategy of an anion-conducting block copolymer to prepare durable ionomers for use in alkaline membrane fuel cells (AMFCs). Our goal was to use new ionomers and binders with an aim at improving long-term stability of AMFCs, especially at high operation temperatures. At 80 °C, AMFCs with *in-situ* cross-linked ionomers showed promising stability with an operating life time of more than 350 hours at 100 mA/cm^2. We found that the optimized electrode fabrication process and operating conditions can significantly improve the durability performance of AMFCs. For example, a suitable electrode binder in addition to the ion-conducting ionomer can greatly enhance the durability performance of AMFCs. Operating fuel cells under a cathode over-humification condition can also enhance the long-term stability of AMFCs.

1. Introduction

There is great demand for the development of efficient, safe and affordable power conversion systems for hybrid, plug-in and full electric vehicles and other mobile and portable power applications [1]. Advanced Li-ion batteries, metal-air batteries (such as Li-air batteries) and proton exchange membrane fuel cells (PEMFCs) are three potential candidates to power future electric vehicles [1–3]. PEMFCs based on a solid polymer proton exchange membrane (PEM) as the electrolyte have attracted intense focus during the past several decades due to their rapid startup, high energy efficiency and high power and energy densities [3–6]. Moreover, compared to the serious range limitations with most battery technologies, fuel cells enable long-range (>500 km) vehicle applications as an alternative to internal combustion engines [3–6]. Although great progress has been made during the past two decades, PEMFCs' heavy reliance on noble metal electrocatalysts such as Pt and its alloys and the high cost of perfluorinated proton exchange membranes (PEMs) such as Nafion® hamper widespread adoption of PEMFC technologies [7].

Alkaline membrane fuel cells (AMFCs) with anion exchange membranes (AEMs) as the solid polymer electrolyte to facilitate high pH cell operation have garnered recent attention due to their distinct advantages over PEMFCs, namely: (1) non-platinum group metals (non-PGM) can be potentially used as electrocatalysts; (2) non-fluorinated AEMs can cost much less than perfluorinated PEMs and not give off degradation products such as HF, (3) inexpensive materials can be used for the cell components such as bipolar plates (e.g. uncoated stamped metal) due to the less corrosive alkaline environment, and (4) the kinetics of oxygen reduction reaction (ORR) is faster at alkaline pH than in acidic environments [8–10]. AMFCs with polymer membranes also eliminate the durability problem of the formation of carbonate deposits in the electrode from the reaction between CO_2 from the oxidation gas (such as air) and metal cations in the liquid alkaline electrolyte solutions (e.g. KOH), which is one of several problems for liquid alkaline fuel cells [10]. In addition, compared to the traditional liquid electrolyte alkaline fuel cells, AMFCs can borrow design strategies for high performance thin film electrodes and MEAs from PEMFCs and can be operated with differential pressures between the anode and cathode compartments, thus optimizing and improving their performance.

During the past decade, much effort has been devoted to the development of stable, ion-conductive AEMs [11–22] and high performance MEAs [23–25] for AMFCs, and important progress has been achieved [11–25]. A significant challenge for AMFCs is developing an alkaline exchange ionomer for use in the electrocatalyst layer to produce high performance and highly durable MEAs. However, there are only a few reports of detailed ionomer development beyond initial demonstrations [26–30]. In

* Corresponding author. Tel.: +1 814 863 1206; fax: +1 814 863 4848.
E-mail address: cxw31@psu.edu (C.-Y. Wang).

http://dx.doi.org/10.1016/j.electacta.2014.11.055
0013-4686/

state-of-the-art PEMFCs, commercially available Nafion® dispersion with high proton conductivity and high stability, are used to produce MEAs with high output and good long-term operational stability. Similar to near-ubiquitous Nafion® dispersion, a suitable alkaline ionomer should be easy to process and have high hydroxide ion (OH^-) conductivity as well as high alkaline stability at the catalytic interface during device operation. Ionomers with high hydroxide conductivity can facilitate an efficient three-phase boundary for the desired electrochemical reactions which significantly improves the catalyst utilization, and can reduce the ionic transport resistance in the electrocatalyst layer [27]. Highly stable ionomers can greatly extend the lifetime of MEAs and allow for optimization of MEA and cell design for high performance. Stable ionomers should have not only high chemical and thermal stability under fuel cell operating conditions (e.g. 80 °C), but also high mechanical strength and low swelling in water in order to maintain the electrode integrity [21]. However, there is a tradeoff between the ionic conductivity and mechanical stability of the ionomer: to increase the mechanical stability and reduce the swelling of the material, the ion-exchange content (IEC) of the ionomer should be limited to moderate levels, leading to low ionic conductivity; while high ionomer ionic conductivity generally requires high IEC, resulting in poor mechanical stability and severe swelling of the ionomer. One effective solution to this tradeoff is to cross-link the ionomer to facilitate high ion content, but limit swelling [17,20–22,31,32]. For example, Robertson et al. [17] used ring-opening metathesis polymerization to generate new cross-linked membrane materials exhibiting high hydroxide ion conductivity and good mechanical properties and found that cross-linking allows for increased ion incorporation, which in turn supports high conductivities. In another example, Pan et al. grafted a tertiary amino group onto a quaternary ammonium-functionalized polysulfone to obtain a cross-linked membrane by a self-cross-linking process between the tertiary amino group and residual benzyl chlorides on the backbone during membrane casting [20,21]. Their membrane showed good chemical and physical stability, even at 90°C [20]. However, upon cross-linking, the polymer became insoluble and no stable ionomer solution has been demonstrated using this approach for MEA fabrication [20,22].

Like Nafion® or other perfluorinated ionomer dispersions for PEMFCs, an ideal ionomer for AMFCs should have high solubility in water or a low-boiling-point organic solvent such as ethanol, n-propanol or isopropanol to make MEA fabrication process simple and cost-effective [27]. Many electrode fabrication processes rely on having the correct mixture of solvents for fast processing of the electrode and proper formation of the ionomer layer. Most of the ionomers demonstrated to date in cell testing have been non-cross-linked quaternary ammonium or phosphonium containing polymers [26–30]. Those ionomers showed either low hydroxide ion conductivity or poor alkaline stability, leading to low performance or limited lifetime of the MEAs during device testing. Little attention has been paid to the alkaline stability of ionomers in the electrode and long-term stability of MEAs over a few hundred hours [26–30]. It is an especially challenging problem to develop MEAs with both high performance and high long-term stability simultaneously [25].

In this work, we adopted an *in-situ* cross-linking strategy to prepare a cross-linked ionomer during the electrode fabrication process. The *in-situ* cross-linking method was first introduced by Varcoe's group for the fabrication of stable alkaline polymer interface between the electrode and AEM [33,34]. They demonstrated promising performance with a peak power density of ~230 mW/cm^2 at 50 °C with hydrogen and oxygen feeds [34]. They also reported a durability test with a lifetime of 233 h at 50 °C for the MEA in methanol/air mode where the steady-state current was ~0.1 A (or 4 mA/cm^2) and the cell potential was 0.17~0.19 V [33]. In this work, we demonstrate high performance and promising long-term stability for our AMFCs with *in-situ* cross-linked ionomers. Effects of electrode fabrication process and operating conditions on the durability performance of AMFCs will also be reported. Since there are a lot of results in the literature on Pt or Pt/C used as anode/cathode catalysts for AMFCs [23–34], we will adopt Pt/C as our benchmark anode/cathode catalysts in order to compare our materials and processes to those already reported.

2. Experimental

2.1. Synthesis of block copolymer anion-exchange ionomer precursor

All chemicals and reagents were purchased from Sigma-Aldrich (St. Louis, MO) except as noted. Styrene (>99%) was distilled under reduced pressure. Vinylbenzyl chloride (VBC) (>90%) was deinhibited by 0.5 wt.% NaOH solution, and then washed by DI water. 2,2'-Azobis (2-methylpropionitrile) (AIBN) (98%) was purified by recrystallization from methanol. S-dodecyl-S'-(α, α'-methyl-α"-acetic acid) trithiocarbonate (DDMAT) (98%) and N,N,N',N'-tetramethyl-1,6-hexanediamine were used as received.

To synthesize the block copolymer anion exchange ionomer precursor, a stirring mixture of styrene (14.060 g, 0.135 mol), DDMAT (342.0 mg, 0.938 mmol) and AIBN (51.3 mg, 0.312 mmol) was bubbled with argon for 30 min and immersed in a preheated oil bath at 60 °C for 24 h. The reaction solution was quenched by liquid nitrogen for 5 min and warmed to room temperature over 30 min. The reaction mixture was diluted with THF, precipitated three times in a large amount of methanol and then dried *in vacuo* at 40 °C to give the poly(styrene) macroinitiator (Macro-PS_{100}, M_n = 13.0 kg mol^{-1}, M_w/M_n = 1.12, M_{nNMR} = 12.5 kg mol^{-1}) as a yellow solid.

A solution of Macro-PS_{100} (4.578 g, 0.440 mmol), VBC (18.314 g, 120 mmol), and AIBN (32.6 mg, 0.200 mmol,) in benzene (10 mL) was degassed by argon sparging for 30 min and placed in a preheated oil bath at 70 °C for 11 h. Purification of the resulting polymer was carried out in a similar fashion to Macro-PS_{100} to give PS_{100}-b-$PVBC_{167}$ (M_n = 18.0 kg mol^{-1}, M_w/M_n = 1.20) as a light yellow solid. The average degree of polymerization of the PVBC block was calculated from the molar ratio of PVBC to PS monomer residues based on the aromatic protons (-C_6H_4- and -C_6H_5-) to chloromethyl protons ($ClCH_2$-) in the ^{1}H NMR spectrum.

^{1}H and ^{13}C nuclear magnetic resonance (NMR) spectroscopy were performed on a Bruker (Bruker Biospin, Billerica, MA) CDPX-300 or DRX-400 FT-NMRs using $CDCl_3$ as solvent and the residue peaks of $CDCl_3$ as internal references. Gel permeation chromatography (GPC) was conducted to determine the molecular weight and polydispersity index and calibrated with polystyrene standards (Varian, Lake Forest, CA) in tetrahydrofuran (THF) with a flow rate of 1 mL min^{-1} at 35 °C on a Waters (Milford, MA) GPC system with a Waters 2414 refractive index (RI) detector. Synthesized ionomer precursors were then dissolved in ethyl acetate for electrode fabrication.

2.2. Electrode fabrication and in-situ ionomer quaternization

The catalyst-coated substrate (CCS) method was adopted to prepare two types of electrodes: the first type of CCS electrode was an ionomer precursor self-bonded electrode that was quaternized after electrode deposition; and the other type of electrode was a Nafion-bonded electrode, followed by the impregnation of ionomer precursor solution into the bonded electrode structure and then quaternization. In the case of self-bonded electrode, 46 wt. % Pt/C catalyst (TKK, Japan) was mixed with water, 1-propanol and in-house synthesized ionomer precursor solution (5 wt. % in ethyl acetate) to obtain a well-dispersed ink under magnetic stirring combined with

15 min ultra-sonication. To obtain a CCS, the as-prepared ink was sprayed onto the surface of SIGRACET® GDL 25BC carbon paper substrate (SGL Carbon Group, Germany) using an air spray gun (Iwata, Japan). In the self-bonded electrocatalyst layer, the catalyst loading was ~0.5 g/cm^2 Pt, and the content of ionomer precursor was ~20 wt. %. In the case of Nafion®-bonded electrode, 46 wt.% Pt/C catalyst (TKK, Japan) was mixed with water, isopropanol and 5 wt.% Nafion® solution (here used as the binder) to obtain a well-dispersed ink using a similar mixing method as above. The as-prepared ink was also sprayed onto the surface of SIGRACET® GDL 25BC carbon paper substrate (SGL Carbon Group, Germany) to obtain a CCS. The catalyst loading was ~0.5 g/cm^2 Pt, and the Nafion® binder content was 10 wt. % in the Nafion-bonded electrocatalyst layer. After initial electrode layer deposition, in-house synthesized ionomer precursor solution (1 wt. % in ethyl acetate) was then sprayed onto the surface of Nafion-bonded electrocatalyst layer until the required ionomer precursor mass loading was achieved. The loading of ionomer precursor in the Nafion-bonded electrocatalyst layer was ~22 wt. %.

The precursor form ionomer was quaternized, *in-situ*, by immersing the as-prepared electrode (either self-bonded or Nafion®-bonded) in N, N, N', N'-tetramethyl-1, 6-hexanediamine overnight using the method reported by Varcoe, et al. [33,34]. During this treatment, the ionomer precursor was cross-linked by the reaction of the diamine and the ionomer precursor. The reaction is very fast and along with the polymeric nature of the precursor one would not anticipate leaching. The treated electrode was then washed completely with water, soaked in 1 M aqueous $KHCO_3$ solution for at least 5h to convert the chloride-form of *in-situ* synthesized ionomer into bicarbonate form, and finally washed completely with water to remove any residual $KHCO_3$. The pre-treated CCS was cut into ~ 5 cm^2 (2.25 cm × 2.25 cm) for use.

2.3. Fuel cell performance/durability evaluation

For AMFC performance evaluation, A201 membrane with a thickness of 28 μm (Tokuyama Corporation, Japan) was used as the anion exchange membrane (AEM). Prior to the assembly of the AMFC, the AEM was subjected to $KHCO_3$ pre-treatment. In the pre-treatment step, the AEM was soaked in 1 M aqueous $KHCO_3$ solution overnight, and then was washed completely with water to remove residual $KHCO_3$. The pre-treated AEM was then sandwiched with a pair of pre-treated CCS's to form the CCS-AEM-CCS assembly, i.e. the MEA. The MEA was placed in a 5 cm^2 graphite single fuel cell (Fuel Cell Technologies Inc. US) with single-path serpentine flow channel, and the cell fixture was tightened with mechanical fasteners to ensure intimate contact among the layers in the test cell.

AMFC evaluation was performed with a commercial fuel cell test station (Teledyne Energy System Inc. US) including control system, frequency response analyzer, software, anode and cathode humidifiers and electronic load. The AMFC performance was measured at both 50 °C and 80 °C, while the durability test was run at 80 °C. Fully-humidified (i.e. 100% relative humidity (RH)) hydrogen was supplied into the anode as fuel at a specified flow rate in the range of 0.2~2.0 L/min (STP), while fully-humidified (i.e. 100% RH) or over-humidified (i.e. humidifier temperature is higher than cell temperature) oxygen was supplied into the cathode as oxidant at a specified flow rate (typically, 0.2L/min (STP)). The assembled AMFC was pre-activated at 50°C with H_2/O_2 by increasing the current density step by step [24,25]. During the activation process, a set current density was applied until the corresponding cell voltage stabilized; and then increased current density was applied in a further step-wise fashion for MEA activation. After complete activation, the steady-state polarization curves (cell voltage vs. current density) under different operating conditions (such as different gas flow rates, temperatures and humidifier temperatures) were measured in galvanostatic mode. The control of operating parameters and data collection were accomplished with the accompanying test station software. Both steady-state cell voltage and high frequency resistance (HFR) (measured with on-board frequency response analyzer under a frequency of 2kHz) as a function of current density were recorded. For durability testing, a constant current density of 100 mA/cm^2 was applied, and then both steady-state cell voltage and HFR as a function of test time were recorded. The net water transport coefficient (α) through the AEM from the anode to the cathode as a function of test time was also monitored. Net water transport coefficient was measured with our previously reported method for direct methanol fuel cells (DMFCs) [35,36] and polymer electrolyte fuel cells (PEFCs) [37].

3. Results and discussion

3.1. Effect of electrode binder

When the electrodes are exposed to air or soaked in $KHCO_3$ solution, the OH^- as counter ion in the AEM and the ionomer is converted to HCO_3^-/CO_3^{2-}. Before activation, the existence of HCO_3^-/CO_3^{2-} as counter ion reduced the ionic conductivity of the AEM and the ionomer, therefore, the initial performance of MEA was poor. Activation process is necessary to change the ions back to OH^-. During the activation process, after the current density was increased gradually, with the generation of OH^-, HCO_3^-/CO_3^{2-} was purged and released as CO_2 from the anode [38,39]. After complete activation process, the MEA performance significantly increased since the CO_3^{2-} ratio in the AEM and the ionomer was significantly reduced, and then steady-state initial performance of MEA was measured. Fig. 1 shows the cell voltage and power density as a function of current density at 50 °C for the MEAs with self-bonded and Nafion®-bonded electrodes. Note that in the case of MEA with Nafion®-bonded electrodes, Nafion® serves as a binder. After soaking the electrode in 1 M $KHCO_3$ solution, the Nafion® has been converted from H^+- to K^+-form. After conversion, K^+-form Nafion® is not proton conductor, but acts as an ionic mechanical binder. In the literature, Nafion® was adopted as a binder to fabricate thin film rotating disk electrodes (RDE) with catalyst nanoparticles for evaluation of electrocatalytic activity in alkaline liquid electrolyte solution (such as KOH) [40,41]. For both MEAs, when increasing the anode gas flow rate, the peak power density increased significantly. However, when increasing the cathode gas flow rate, the peak power density did not change appreciably. For example, for the MEA with Nafion®-bonded electrodes, when the hydrogen flow rate was increased from 200 to 2000 std. cm^3/min (SCCM) (and the oxygen flow rate was kept constant at 200 SCCM), the peak power density increased significantly from 41 to 144 mW/cm^2; but when the oxygen flow rate was increased from 200 to 1000 SCCM (and the hydrogen flow rate was held constant at 2000 SCCM), the peak power density remained virtually unchanged, with a slight increase from 144 to 147 mW/cm^2. For AMFCs, water is consumed at the cathode side, while water is generated in the anodic reaction. Therefore, electrode flooding may occur at the anode. From Fig. 1, for both MEAs with self-bonded and Nafion®-bonded electrodes, when the anode gas flow rate was low (such as 200 SCCM), the MEA performance was poor due to anode flooding, as evidenced by the low limiting current density (<250 mA/cm^2) and small peak power density under these conditions. Increasing the anode gas flow rate can effectively remove the water accumulated at the anode, thus boosting the MEA performance and increasing the peak power density. At 50 °C, when the hydrogen and oxygen flow rates were 2000 and 200 SCCM, respectively, the peak power density was ~144 mW/cm^2 for the MEA with Nafion®-bonded electrodes, which was higher than the peak power density observed for the MEA with self-bonded electrodes (~ 96 mW/cm^2).

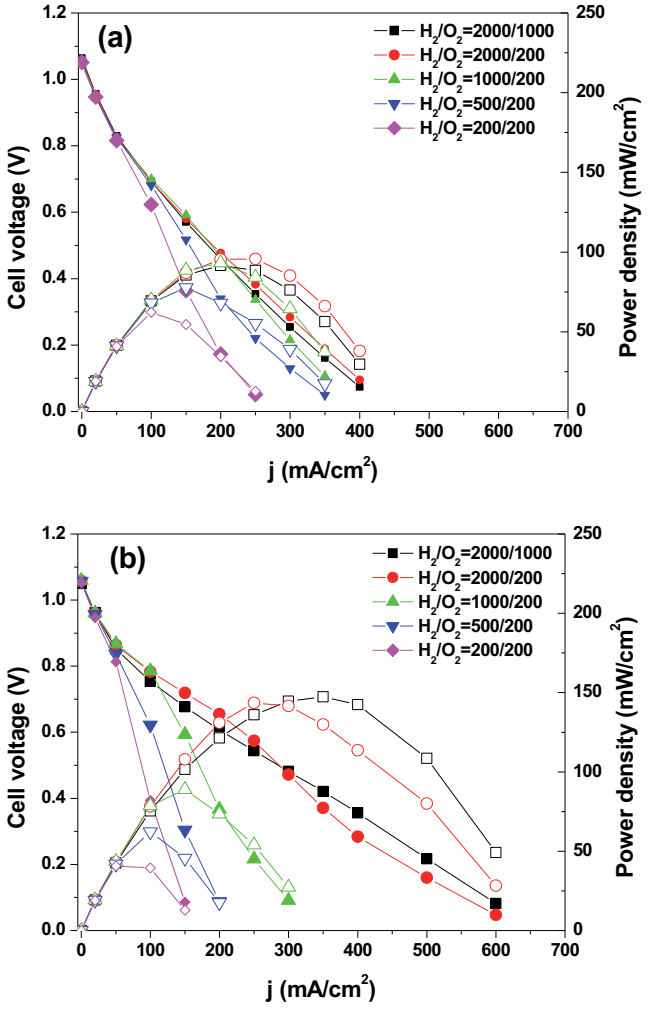

Fig. 1. Cell voltage and power density as a function of current density at 50 °C under different anode/cathode flow rates (flow rate in units of SCCM) for MEAs with (a) self-bonded and (b) Nafion®-bonded electrodes. Anode/cathode humidifier temperature: 50 °C.

At 50 °C, for the MEA with Nafion®-bonded electrodes, a maximum peak power density of 147 mW/cm^2 was achieved when the hydrogen and oxygen flow rates were 2000 and 1000 SCCM, respectively. The maximum peak power density achieved at 50 °C in this work was slightly lower than ~160 mW/cm^2 peak power density obtained at the same temperature for an MEA with a 38 μm thick membrane, Teflon-bonded Pt/C electrodes and cross-linked alkaline polymer interface between the electrode and AEM by Varcoe et al. [34], while was much higher than the reported value (<55 mW/cm^2) at the same temperature by Luo et al. [32] for an MEA with QPMBV ionomer (i.e. quaternized poly(methyl methacrylate-co-butyl acrylate-co-vinylbenzyl hydroxide)). In addition, the maximum peak power density achieved at 50 °C in this work was comparable to the peak power of ~138 mW/cm^2 obtained by Gu et al. [27] for an MEA with TPQPOH ionomer (i.e. tri(2,4,6-trimethoxyphenyl)-pulsulfone-methylene quaternary phosphonium hydroxide). One can estimate the total cell resistance from the slope of polarization curve (i.e. cell voltage vs. current density (j)), which includes the contributions of ohmic resistance, the resistance of ionic transport in the electrocatalyst layer, and the mass transport resistance. For example, in the case of the self-bonded MEA, from the slope of polarization curve shown in Fig. 1a, the total resistance was estimated to be 2.5 Ω cm^2 under H_2/O_2 = 2000/200 SCCM, which was much higher than our observed HFR (~1.0 Ω cm^2, not shown here). It is also found that under the same cathode flow rate of 200 SCCM, with increasing the anode flow rate from 200 to 2000 SCCM, HFR increased slightly (from ~0.84 to ~1.04Ω cm^2, not shown here), but the total resistance obtained from the slope of the polarization curve decreased significantly. This is mainly due to a significant decrease of mass transport resistance of H_2 at the anode with increasing H_2 flow rate, leading to a large decrease of total resistance and an improved MEA performance.

We compared the power density and high-frequency resistance (HFR) as a function of current density at 80 °C for the MEAs with self-bonded and with Nafion-bonded electrodes, as shown in Fig. 2. For the MEA with Nafion-bonded electrodes, the peak power density was 156 and 172 mW/cm^2 when the H_2/O_2 gas flow rates were 100/100 and 200/200 SCCM, respectively; higher than 111 and 116 mW/cm^2 at the same gas flow rates for the MEA with self-bonded electrodes. We also found that for the MEA with Nafion-bonded electrodes, the HFR at 80 °C was in the range of 0.37~0.53 ohm cm^2, much lower than that (i.e. 0.74~0.90 ohm cm^2) observed for the MEA with self-bonded electrodes. This result indicates that Nafion-bonding can effectively bridge catalyst particles and *in-situ* cross-linked ionomers to increase intimate contact between the catalyst particles and ionomers. Nafion® as a binder may also impart good mechanical stability to the electrode, which reduces the contact resistance, leading to higher MEA

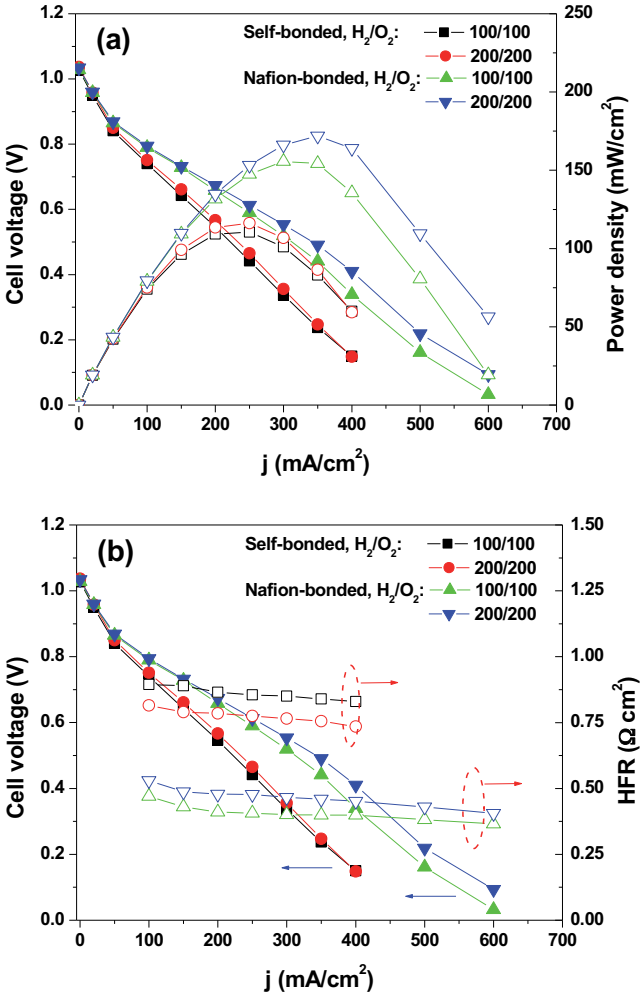

Fig. 2. (a) Power density and (b) high-frequency resistance (HFR) as a function of current density at 80 °C with balanced anode/cathode flow rates (flow rate in units of SCCM) for MEAs with self-bonded electrodes or Nafion®-bonded electrodes. Anode/cathode humidifier temperature: 80 °C.

performance in the case of MEA with the Nafion®-bonded electrodes. Too much swelling of self-bonded electrodes and poor mechanical properties can result in the high observed HFRs. In the case of MEA with Nafion®-bonded electrodes, Nafion may be animated with N, N, N', N'-tetramethyle-1, 6-hexanediamine, and thus animated Nafion can be also acted as an additional anion conductor besides the binder function [42].

A critical concern for alkaline membrane fuel cell technology is durability during device operation. It has been well-documented that most AEMs suffer from poor chemical stability [8,10,43]. It is reported that nucleophilic attack on the cationic fixed charged sites by OH^- was the main reason for chemical degradation of AEMs [10]. This kind of degradation leads to a loss in the number of anion-exchange groups and thus a decrease in hydroxide ion conductivity [10]. Since the ionomer used in the catalyst layer is in intimate contact with the catalyst surface, the chemical or electrochemical degradation of the ionomer may be more severe than that of the membrane [44]. Due to the lack of a stable ionomer, especially at high temperatures (such as 80 °C), only a few reports on the long-term stability of AMFCs at low temperatures (such as 50 °C) have been published, while little work has been reported at high temperatures [23–34]. For example, Piana et al. [23] demonstrated a lifetime of 320 h for an MEA with a proprietary ionomer operated at 50 °C; and Lim et al. [24] reported ~120 h lifetime for MEA with AS-4 ionomer (Tokuyama Corporation) at 50 °C. Luo et al. [32] demonstrated lifetimes of ~420 and ~150 h at 50 and 70 °C, respectively, for an MEA with QPMBV ionomer and a cross-linked AEM. Since our cross-linked ionomer showed reasonable alkaline stability in 1 M KOH solution at 80 °C during *ex-situ* testing, we explored the long-term stability of AMFCs with *in-situ* cross-linked ionomer at high cell temperatures. Fig. 3 shows the durability performance of MEAs with self-bonded and Nafion®-bonded electrodes at 80 °C. The purpose of high temperature operation in this work was to accelerate the MEA durability test under severe conditions and evaluate the stability of MEAs with *in-situ* cross-linked ionomer at high temperatures. As shown in Fig. 3, the *in-situ* cross-linked ionomer can tolerate high temperatures and the MEA with *in-situ* cross-linked ionomer can be stably operated at high temperature for several hundred hours. The MEA with self-bonded electrodes showed a lifetime of ~114 h at 80 °C. Interestingly, the MEA with Nafion-bonded electrodes and impregnated cross-linked ionomer showed much better durability performance with a lifetime of 269 h, which was more than double

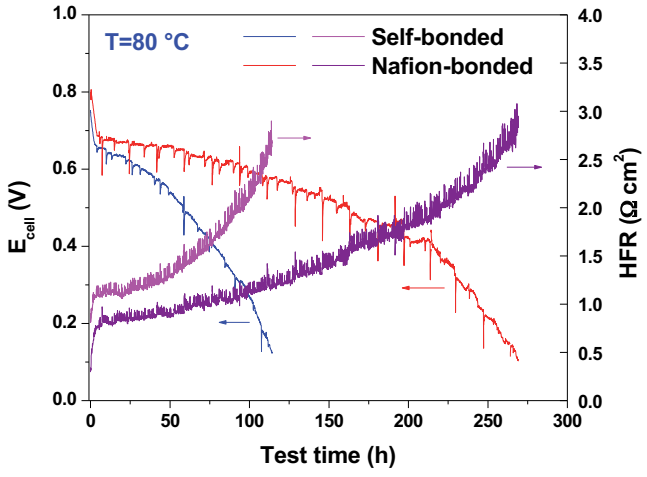

Fig. 3. Cell voltage and HFR as a function of test time under a constant current density of 100 mA/cm^2 at 80 °C for MEAs with self-bonded electrodes and with Nafion®-bonded electrodes. Anode/cathode flow rates were 200/200 SCCM. Anode/cathode humidifier temperature: 80 °C.

lifetime for the MEA with self-bonded electrodes. We believe that Nafion® bonding can maintain better electrode mechanical integrity and more intimate contact between the catalyst particles and the ionomer during durability testing, leading to superior long-term performance. The HFR of the MEA with Nafion®-bonded electrodes increased with durability test time at a much lower rate compared to the HFR increase of the MEA with self-bonded ionomer electrodes. The lifetime obtained at 80 °C for the MEA with Nafion®-bonded electrodes in this work was greater than ~150 h at 70 °C achieved by Luo et al. [32] for an MEA with QPMBV ionomer and a cross-linked AEM. This result suggested that our *in-situ* cross-linked ionomer has excellent alkaline stability at high temperature compared with a non-cross-linked ionomer.

3.2. Effect of cathode relative humidity (RH)

Another important issue related to AMFC operation is water management. Since water is generated at the anode side and consumed at the cathode side, water management may be more critical for AMFCs than for PEMFCs [45]. If the water cannot be properly managed, anode-flooding and cathode dry-out may occur. Proper water management in AMFCs may not only improve MEA performance but also extend cell lifetime since the hydration state of the cell has a large effect on MEA stability and water is known to stabilize the ion-containing polymers in AMFCs [46]. Before we develop strategies for water management, we need to know the net water flux through the AEM from the anode to the cathode under different operating conditions and MEA configurations, and we also need to monitor the change of net water flux during durability testing. The net water flux (in mol/s) transported from the anode to the cathode through AEM can be expressed as:

$$N_{trans,w} = \alpha \times \frac{IA}{F} \quad (1)$$

where α is the net water transport coefficient, I is the current density, A is the electrode active area, and F is Faraday's constant. For AMFCs, in general, since water is generated at the anode and consumed at the cathode, water will diffuse through the AEM from anode to cathode under the water concentration gradient. However, due to the effect of electro-osmotic drag, water will be transported back from cathode to anode accompanying the transport of the hydroxide ion. The direction of net water flux transportation through the AEM depends on a combined result of electro-osmotic drag (EOD) and water diffusion through the AEM under a certain operation condition [45,47], similar to the cases of a DMFC [35,36] or a PEMFC [37]. Positive α means a net water flux from the anode to the cathode; while negative α indicates a net water flux from the cathode to the anode. The net water transport coefficient (α) can be obtained using the water balance equation at the anode side as follows:

$$N_{inlet} + N_{power,w} = N_{outlet} + \alpha\frac{IA}{F} \quad (2)$$

where, N_{inlet}, $N_{power,\ w}$, and N_{outlet} are the water flux at the inlet, water produced from power generation at the anode and water flux at the outlet, respectively.

In the operation of an AMFC, humidified hydrogen is fed into the anode, where hydrogen is oxidized electrochemically via:

$$H_2 + 2OH^- \rightarrow 2H_2O + 2e^- \quad (3)$$

The water produced from power generation can thus be described as:

$$N_{power,w} = \frac{IA}{F} \quad (4)$$

Once we know the water flux at the inlet and the outlet, the net water transport coefficient can be measured according to:

$$\alpha = (N_{let} - N_{outlet}) \times \frac{F}{IA} + 1 \quad (5)$$

We measured the net water transport coefficient for both MEAs with self-bonded electrodes and with Nafion®-bonded electrodes during the durability test, as shown in Table 1. In the case of the MEA with self-bonded electrodes, after durability testing for 17 h, the net water transport coefficient (α) was -0.227 at 80 °C under both anode and cathode RH of 100%. In the case of the MEA with Nafion®-bonded electrodes, at 80 °C under both anode and cathode RH of 100%, the net water transport coefficient (α) was -0.367 and -0.245 after durability testing for 15 h and 232 h, respectively. These results indicated that the net water flux through the AEM was from cathode to anode at 80 °C for both cases, which is quite different from the case at low temperatures such as 50 °C. Zhang et al. [45] observed that in a solid-state alkaline fuel cell with pore-filling electrolyte, at 50 °C, the net water transports from the anode to the cathode, since the water that transports from the anode to the cathode via water diffusion is more than the water accompanies with ionic flux from the cathode back to the anode via EOD. Our group also observed net water movement from the anode to the cathode for AMFCs operated at 50 °C [47]. However, at high temperatures, the EOD coefficient of an AEM may increase with increasing operating temperature, like the case in a PEMFC [48]. If the effect of electro-osmotic drag is dominant at high temperatures, the net water flux may be from the cathode to the anode in the case of an AMFC.

Since water is consumed at the cathode and the net water flux through the AEM was from cathode to anode at high temperatures, cathode dry-out may occur. The dry-out will lead to low hydroxide ion conductivity of the ionomer in the cathode catalyst layer and the AEM, causing high ion transport resistance in the electro-catalyst layer, low catalyst utilization, and high membrane resistance. Supplying more water into the cathode side is helpful to alleviate cathode dry-out. It will not only increase initial MEA performance, but also improve MEA durability. Fig. 4 shows a comparison of the power density and cell HFR as a function of current density at 80 °C for another fresh MEA with Nafion-bonded electrodes for two cathode humidification conditions: 100% cathode relative humidity (RH) (i.e. cathode humidifier temperature was 80 °C, equal to the cell temperature); and cathode over-humidification (i.e. cathode humidifier temperature was 83 °C, higher than the cell temperature). As shown in Fig. 4, the power density of the MEA operated under cathode over-humidification was 152~154 mW/cm^2, which was higher than the 135~136 mW/cm^2 under 100% cathode RH condition. The HFR of the MEA under cathode over-humidification was 0.33~0.38 Ω cm^2, lower than 0.44~0.56 Ω cm^2 of the MEA under 100% cathode RH condition. For the MEA operated under cathode over-humidification condition, with more water supplied into the cathode, a more highly hydrated ionomer in the cathode catalyst layer would be expected, leading to higher ionic conductivity of the ionomer and lower HFR.

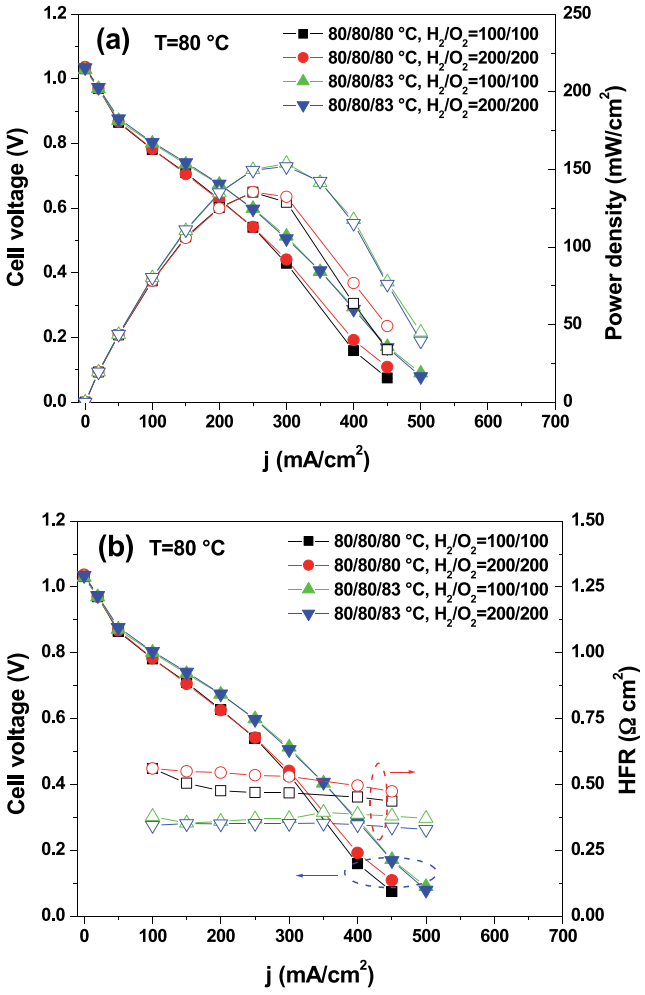

Fig. 4. A comparison of (a) power density and (b) high-frequency resistance (HFR) as a function of current density at 80 °C for the MEA with Nafion®-bonded electrodes operated under 100% cathode RH (cathode humidifier temperature: 80 °C) and under cathode over-humidification (cathode humidifier temperature: 83 °C) conditions. (Note: 80/80/80 °C means that anode humidifier, cell and cathode humidifier temperatures are 80, 80 and 80 °C, respectively; while 80/80/83 °C means that anode humidifier, cell and cathode humidifier temperatures are 80, 80 and 83 °C, respectively.)

Besides the MEA performance, it is interesting to explore the effects of cathode over-humidification on the long-term stability of the cell. We did find that operating the MEA under cathode over-humidification condition can extend its lifetime for the MEA with Nafion-bonded electrodes, as shown in Fig. 5. The MEA operated under cathode over-humidification condition demonstrated a lifetime of ~356 h, which was higher than that (~269 h) under 100% cathode RH. Compared to the 100% cathode RH case, the testing with an over-humidified cathode also showed a lower HFR and a slower rate of HFR increase with durability test time. These results suggested that the ionomer stability may be related to the hydration (i.e. water content) of the ionomer in the electro-catalyst

Table 1
Water transport coefficient (α) during durability testing for the MEAs with self-bonded and Nafion®-bonded electrodes.

Case No.	Sample	Operating condition[a]	Water transport coefficient (α)
Case 1	MEA with self-bonded electrodes	T = 80 °C Anode humidifier: 80 °C Cathode humidifier: 80 °C	t = 17 h, α = -0.227
Case 2	MEA with Nafion®-bonded electrodes	T = 80 °C Anode humidifier: 80 °C Cathode humidifier: 80 °C	t = 15 h, α = -0.367 t = 232 h, α = -0.245
Case 3	MEA with Nafion®-bonded electrodes	T = 80 °C Anode humidifier: 80 °C Cathode humidifier: 83 °C	t = 16 h, α = -1.493 t = 232 h, α = -1.409

[a] Operating conditions were: cell temperature of 80 °C, H_2/O_2 flow rates of 200/200 SCCM, current density of 100 mA/cm^2.

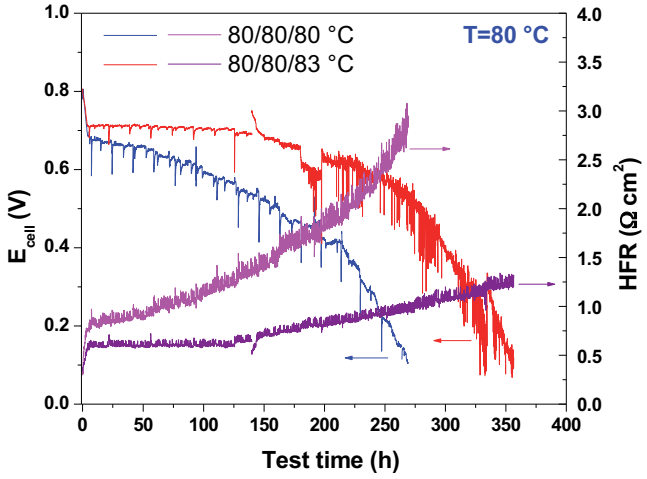

Fig. 5. Cell voltage and HFR as a function of test time under a constant current density of 100 mA/cm^2 at 80 °C for the MEA with Nafion®-bonded electrodes operated under two different cathode humidification conditions: (a) 100% RH (cathode humidifier temperature: 80 °C); (b) over-humidification (cathode humidifier temperature: 83 °C). Anode/cathode flow rates: 200/200 SCCM.

layer. This result opens a new window for improving the ionomer stability by proper water management in an operating device. The net water transport coefficient was measured during durability testing, as shown in Table 1. After durability testing for 16 h, for the MEA with Nafion-bonded electrodes operated under cathode over-humidification (Case 3 in Table 1), the net water transport coefficient (α) was -1.493, much smaller than that for the same MEA operated under 100% cathode RH (Case 2 in Table 1). This result indicated that more water was transported through the AEM from the cathode to the anode under cathode over-humidification condition. For the MEA operated under cathode over-humidification condition, since excess water was supplied into the cathode, the water concentration gradient between the anode and the cathode became smaller, leading to much less water diffusion from the anode to the cathode. Considering the electro-osmotic drag effect was similar for both cases, much less water diffusion from the anode to the cathode led to larger net water flux from the cathode to the anode when MEA was operated under cathode over-humidification condition. With increasing durability test time from 16 to 232 h, the net water transport coefficient for the MEA operated under cathode over-humidification condition changed from -1.493 to -1.409. This kind of change may be related to the change of the hydrophobicity/hydrophilicity of the anode and cathode gas diffusion media [49,50]. Note that over-humidification in a practical fuel cell increases operating cost and system complexity. For practical use, in order to avoid cathode dry-out and achieve sufficient water content in the cathode, an innovative and suitable strategy is needed to transport more water produced at the anode from the anode through the AEM to the cathode, for example, using different types of gas diffusion layers with tailored hydrophobic/hydrophilic properties at the anode and cathode.

4. Conclusions

We adopted an *in-situ* strategy to prepare cross-linked ionomers in the electrocatalyst layer for AMFCs. The *in-situ* cross-linked ionomer demonstrated high stability for temperatures up to 80 °C in this work. The MEA with *in-situ* cross-linked ionomer self-bonded electrodes was operated steadily for ~114 h at 80 °C. We found that optimized electrode fabrication process can significantly improve the durability performance of AMFCs. The electrode binder plays an important role in improving the durability performance of AMFCs. For example, the MEA with Nafion®-bonded electrodes and *in-situ* cross-linked ionomer demonstrated excellent durability performance with a lifetime of ~269 h at 80 °C, more than double the ~114 h lifetime measured for the MEA with ionomer self-bonded electrodes. We also found that at 80 °C, the net water flux through AEM was from the cathode to the anode. We confirmed that supplying more water into the cathode can avoid cathode dry-out, increase the hydration of the ionomer, and thus not only increase the MEA performance, but also extend its lifetime. The results presented in the current work provide guidelines for further improvement of long-term stability of AMFC devices. However, our results, as well as most of results reported in literature, are still much lower than those of PEMFCs, which are insufficient for immediate commercialization of AMFCs. AEM fuel cells are still in the early stages of development, and their performance and durability need to be improved significantly. In order to develop highly efficient, durable and low-cost AEM fuel cells, future focus should be placed on: (a) development of easily processible stable ionomers with high ionic conductivity and low cost, (b) development of low cost AEMs with high ionic conductivity, high alkaline stability and high mechanical stability, (c) development of highly active and durable catalysts, especially non-precious group metal catalysts, and (d) fundamental understanding of degradation mechanism of AEM and ionomer used in AEM fuel cells.

Acknowledgement

This work was funded in part by the Advanced Research Projects Agency – Energy (ARPA-E), U.S. Department of Energy, under award number: DE-AR0000121.

References

[1] (a) R. Etacheri, R. Marom, G. Elazari, Challenges in the development of advanced Li-ion batteries: a review, Energy Environ. Sci. 4 (2011) 3243; (b) M.M. Thackeray, C. Wolverton, E.D. Isaacs, Electrical energy storage for transportation— approaching the limits of, and going beyond, lithium-ion batteries, Energy Environ. Sci. 5 (2012) 7854.
[2] J.S. Lee, S.T. Kim, R. Cao, N.S. Choi, M.L. Liu, K.T. Lee, J. Cho, Metal–air batteries with high energy density: Li–air versus Zn–air, Adv. Energy Mater. 1 (2011) 34.
[3] R. Borup, J. Meyers, B. Pivovar, Y.S. Kim, R. Mukundan, N. Garland, D. Myers, M. Wilson, F. Garzon, D. Wood, P. Zelenay, K. More, K. Stroh, T. Zawodzinski, J. Boncella, J.E. McGrath, M. Inaba, K. Miyatake, M. Hori, K. Ota, Z. Ogumi, S. Miyata, A. Nishikata, Z. Siroma, Y. Uchimoto, K. Yasuda, K. Kimijima, N. Iwashita, Scientific aspects of polymer electrolyte fuel cell durability and degradation, Chem. Rev. 107 (2007) 3904.
[4] C.Y. Wang, Fundamental models for fuel cell engineering, Chem. Rev. 104 (2004) 4727.
[5] H.A. Gasteiger, S.S. Kocha, B. Sompalli, F.T. Wagner, Activity benchmarks and requirements for Pt, Pt-alloy, and non-Pt oxygen reduction catalysts for PEMFCs, Appl. Catal. B 56 (2005) 9.
[6] M.A. Hickner, H. Ghassemi, Y.S. Kim, B.R. Einsla, J.E. McGrath, Alternative polymer systems for proton exchange membranes (PEMs), Chem. Rev. 104 (2004) 4587.
[7] (a) R. Bashyam, P. Zelenay, A class of non-precious metal composite catalysts for fuel cells, Nature 443 (2006) 63; (b) K.P. Gong, F. Du, Z.H. Xia, M. Durstock, L.M. Dai, Nitrogen-doped carbon nanotube arrays with high electrocatalyticectivity for oxygen reduction, Science 323 (2009) 760.
[8] J.R. Varcoe, R.C.T. Slade, Prospects for alkaline anion-exchange membranes in low temperature fuel cells, Fuel Cells 5 (2005) 187.
[9] S. Lu, J. Pan, A. Huang, L. Zhuang, J.T. Lu, Alkaline polymer electrolyte fuel cells completely free from noble metal catalysts, Proc. Natl. Acad. Sci. U. S. A 105 (2008) 20611.
[10] C.G. Arges, V. Ramani, P.N. Pintauro, 2010. Anion exchange membrane fuel cells, The Electrochemical Society Interface Summer 31.
[11] G. Merle, M. Wessling, K. Nijmeijer, Anion exchange membranes for alkaline fuel cells: A review, J. Mem. Sci. 377 (2011) 1.
[12] G. Couture, A. Alaaeddine, F. Boschet, B. Ameduri, Polymeric materials as anion-exchange membranes for alkaline fuel cells, Progr. Poly. Sci. 36 (2011) 1521.
[13] J.R. Varcoe, R.C.T. Slade, E.L.H. Yee, S.D. Poynton, D.T. Driscoll, D.C. Apperley, Poly(ethylene-co-tetrafluoroethylene)-derived radiation-grafted anion-exchange membrane with properties specifically tailored for application in

metal-cation-free alkaline polymer electrolyte fuel cells, Chem. Mater. 19 (2007) 2686.
[14] M.R. Hibbs, C.H. Fujimoto, C.J. Cornelius, Synthesis and characterization of poly (phenylene)-based aion exchange membranes for alkaline fuel cells, Macromolecules 42 (2009) 8316.
[15] N.W. Li, Y.J. Leng, M.A. Hickner, C.Y. Wang, Highly stable anion conductive, comb-shaped copolymers for alkaline fuel cells, J. Am. Chem. Soc. 135 (2013) 10124.
[16] J. Yan, M.A. Hickner, Anion exchange membranes by bromination of benzylmethyl-containing poly(sulfone)s, Macromolecules 42 (2010) 2349.
[17] N.J. Robertson, H.A. Kostalik, T.J. Clark, P.F. Mutolo, H.D. Abruna, G.W. Coates, Tunable high performance cross-linked alkaline anion exchange membranes for fuel cell applications, J. Am. Chem. Soc. 132 (2010) 3400.
[18] Q. Zhang, S. Li, S. Zhang, A novel guanidinium grafted poly(aryl ether sulfone) for high-performance hydroxide exchange membranes, Chem. Commun. 46 (2010) 7495.
[19] M. Tanaka, K. Fukasawa, E. Nishino, S. Yamaguchi, K. Yamada, H. Tanaka, B. Bae, K. Miyatake, M. Watanabe, Anion conductive block poly(arylene ether)s: synthesis, properties and application in alkaline fuel cells, J. Am. Chem. Soc. 133 (2011) 10646.
[20] J. Pan, Y. Li, L. Zhuang, J. Lu, Self-crosslinked alkaline polymer electrolyte exceptionally stable at 90 °C, Chem. Commun. 46 (2010) 8597.
[21] J. Pan, C. Chen, L. Zhuang, J.T. Lu, Designing advanced alkaline polymer electrolytes for fuel cell applications, Acc. Chem. Res. 45 (2012) 473.
[22] S. Gu, R. Cai, Y. Yan, Self-crosslinking for dimensionally stable and solvent-resistant quaternary phosphonium based hydroxide exchange membranes, Chem. Commun. 47 (2011) 2856.
[23] M. Piana, M. Boccia, A. Filpi, E. Flammia, H.A. Miller, M. Orsini, F. Salusti, S. Santiccioli, F. Ciardelli, A. Pucci, H_2/air alkaline membrane fuel cell performance and durability using novel ionomer and non-platinum group metal cathode catalyst, J. Power Sources 195 (2010) 5875.
[24] P.C. Lim, PhD dissertation, Pennsylvania State University, 2009.
[25] K. Fukuta, Electrolyte materials for AMFCs and AMFC performance, Proceedings from the Alkaline Membrane Fuel Cell Workshop, May 8-9, Arlington, Virginia, 2011.
[26] H. Yanagi, K. Fukuta, Anion exchange membrane and ionomer for alkaline membrane fuel cells (AMFCs), ECS Trans. 16 (2008) 257.
[27] S. Gu, R. Cai, T. Luo, Z.W. Chen, M.W. Sun, Y. Liu, G.H. He, Y.S. Yan, A soluble and highly conductive ionomer for high performance hydrogen exchange membrane fuel cells, Angew. Chem. Int. Ed. 48 (2009) 6499.
[28] R. Zeng, J. Handsel, S.D. Poynton, A.J. Roberts, R.C.T. Slade, H. Herman, D.C. Apperley, J.R. Varcoe, Alkaline ionomer with tunable water uptakes for electrochemical energy technologies, Energy Environ. Sci. 4 (2011) 4925.
[29] L. Sun, J. Guo, J. Zhou, Q. Xu, D. Chu, R. Chen, Novel nanostructured high-performance anion exchange ionomers for anion exchange membrane fuel cells, J. Power Sources 202 (2012) 70.
[30] M. Mamlouk, K. Scott, Effect of anion functional groups on the conductivity and performance of anion exchange polymer membrane fuel cells, J. Power Sources 211 (2012) 140.
[31] J.S. Park, S.H. Park, S.D. Yim, Y.G. Yoon, W.Y. Lee, C.S. Kim, Performance of solid alkaline fuel cells employing anion-exchange membranes, J. Power Sources 178 (2008) 620.
[32] Y.T. Luo, J.C. Guo, C.S. Wang, D. Chu, Fuel cell durability enhancement by crosslinking alkaline anion exchange membrane electrolyte, Electrochem. Commun. 16 (2012) 65.
[33] J.R. Varcoe, R.C.T. Slade, E.L.H. Yee, An alkaline polymer electrochemical interface: a breakthrough in application of alkaline anion-exchange membranes in fuel cells, Chem. Commun. (2006) 1428.
[34] J.R. Varcoe, M. Beillard, D.M. Halepoto, J.P. Kizewski, S.D. Poynton, R.C.T. Slade, Membrane and electrode materials for alkaline membrane fuel cells, ECS Trans. 16 (2008) 1819.
[35] F.Q. Liu, G.Q. Lu, C.Y. Wang, Low crossover of methanol and water through thin membranes in direct methanol fuel cells, J. Electrochem Soc. 153 (2006) A543.
[36] G.Q. Lu, F.Q. Liu, C.Y. Wang, Water transport through Nafion 112 membrane in DMFCs, Electrochem. Solid State Lett. 8 (2005) A1.
[37] X.H. Ye, C.Y. Wang, Measurement of water transport properties through membrane-electrode assemblies: Part I. membrane, J. Electrochem. Soc. 154 (2007) B676.
[38] S. Watanabe, K. Fukuta, H. Yanagi, Determination of carbonate ion in MEA during alkaline membrane fuel cell (AMFC) operation, ECS Transactions 33 (1) (2010) 1837.
[39] Z. Siroma, S. Watanabe, K. Yasuda, K. Fukuta, H. Yanagi, Mathematical modeling of the concentration profile of carbonate ions in an anion exchange membrane fuel cell, J. Electrochem. Soc. 158 (6) (2011) B682.
[40] X.G. Li, G. Liu, B.N. Popov, Activity and stability of non-precious metal catalysts for oxygen reduction in acid and alkaline electrolytes, J. Power Sources 195 (2010) 6373.
[41] J. Suntivich, H.A. Gasteiger, N. Yabuuchi, Y. Shao-Horn, Electrocatalytic measurement methodology of oxide catalysts using a thin-film rotating disk electrode, J. Electrochem. Soc. 157 (8) (2010) B1263–B1268.
[42] K. Miyazaki, N. Sugimura, K. Kawakita, T. Abe, K. Nishio, H. Nakanishi, M. Matsuoka, Z. Ogumi, Aminated perfluorosulfonic acid ionomers to improve the triple phase boundary region in anion-exchange membrane fuel cells, J. Electrochem. Soc. 157 (11) (2010) A1153.
[43] B. Bauer, H. Strathmann, F. Effenberger, Anion-exchange membranes with improved alkaline stability, Desalination 79 (1990) 125.
[44] Y.J. Leng, G. Chen, A.J. Mendoza, T.B. Tighe, M.A. Hickner, C.Y. Wang, Solid-state water electrolysis with an alkaline membrane, J. Am. Chem. Soc. 134 (2012) 9054.
[45] H. Zhang, H. Ohashi, T. Tamaki, T. Yamaguchi, Direction and management of water movement in solid-state alkaline fuel cells, J. Phys. Chem. C 116 (2012) 7650.
[46] S. Chempath, B.R. Einsla, L.R. Pratt, C.S. Macomber, J.M. Boncella, J.A. Rau, B.S. Pivovar, Mechanism of tetraalkylammonium headgroup degradation in alkaline fuel cell membranes, J. Phys. Chem. C 112 (2008) 3179.
[47] T. Isomura, K., Fukuta, H., Yanagi, S.H., Ge, C.Y. Wang,2011. Impact of low cathode humidification on alkaline membrane fuel Cell performance, Abstract #221, 219th ECS Meeting, Montreal, QC, Canada.
[48] X.M. Ren, S. Gottesfeld, Electro-osmotic drag of water in poly(perfluorosulfonic acid) membranes, J. Electrochem. Soc. 148 (2001) A87.
[49] F.Q. Liu, C.Y. Wang, Water and methanol crossover in direct methanol fuel cells-effect of anode diffusion media, Electrochim. Acta 53 (2008) 5517.
[50] X.H. Ye, C.Y. Wang, Measurement of water transport properties through membrane-electrode assemblies: Part II. cathode diffusion media, J. Electrochem. Soc. 154 (2007) B683.